
Check for updates

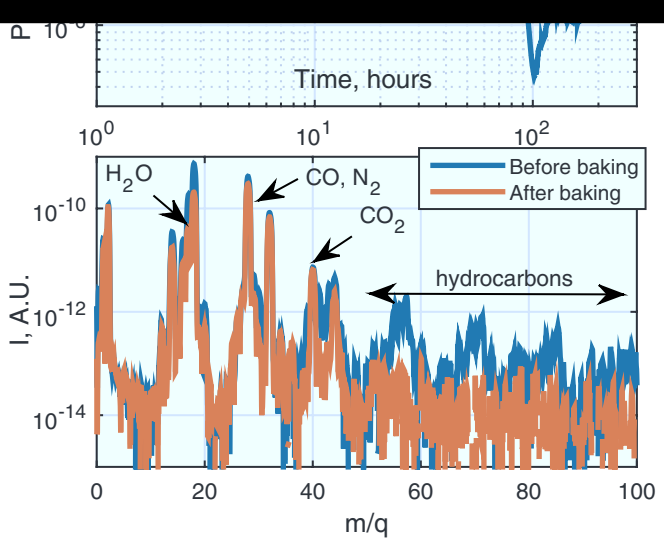

Fig. 1. Baking procedure preceding first plasma operation. Top: vessel temperature in time, including about 1 week at 150 °C. Middle: Pressure decay during 150 °C flat top phase and $t^{-0.7}$ trend curve. Bottom: vacuum QMS spectra before (July 31) and after baking (August 12) at 28 °C.

graphite DC anodes, one per half module, operated at max. 1.5 A per anode [6]. GDC is operated between experimental days when the magnetic field coils are deenergized. H_2-GDC and He-GDC are operated respectively weekly and daily.

2. Initial conditioning

2.1. Baking

One week of baking at 150 °C after the initial pump down of the vacuum vessel prepared the vessel for high vacuum. Heating of the wall materials induces thermal desorption of particles. Quadrupole mass spectrometry (QMS) shows that H_2O is the main outgassed species, with about 10^{25} H_2O molecules removed throughout the procedure. CO and CO_2, the next most prominent molecules, are released at > 10x lower rates. A comparison of continuous QMS mass m over charge q spectra at 28 °C before (blue) and after (red) baking is given in Fig. 1. The footprint of higher hydrocarbons is suppressed while the water content is reduced by one order of magnitude. The pressure curve during the 150 °C temperature plateau follows a typical $t^{-0.7}$ time dependency for outgassing in fusion devices [7] (Fig. 1b). The power law originates from processes such as de-trapping of particles at trapping site concentrations in the PFC, diffusion of those particles through the material bulk and their subsequent recombination to volatile molecules at the surface (Section 4.2). The dependency makes that the relative changes in the neutral pressure scale inversely proportional to time, $1/p\ dp/dt \approx -t^{-1}$, unlike for an exponential decay where latter quantity is

is is
CRH

m tem-
surfaces.
s reduces
metal oxides, hydrogenates the carbon surfaces and forms volatile species that can be evacuated from the vessel [8]. About 10^{23}–10^{24} molecules of CO are removed, estimated from QMS data. Fig. 2 shows QMS intensities for mass m over charge q signals corresponding to CH_4 (m/q = 16), H_2O (18), CO (28), Ar (40), and CO_2 (44) for subsequent H_2-GDC's procedures as function of the cumulated GDC time. The signals are normalized to the applied glow current (1–1.5 A/anode). As chemical sputtering continuously generates CH_4 its signal saturates in time. The expected $t^{-0.7}$ outgassing trend for other impurities is added as multiple black dashed lines. The stronger partial pressure decay in the first 50 s results from the step-by-step increase of the pumping speed to the maximum value and subsequent step-by-step decrease of the gas flow. The gas flow was doubled after this optimization procedure, which explains the observed partial pressure discontinuity at that time. The increased partial pressures at 650 s are consequent to an air leak that preceded the GDC, and that led to an increased torus pressure of 5×10^{-5}mbar within 5 h.

The vertical red dashed lines indicate ECRH operation days, with discharges in H_2 and He, which are typically preceded by 20–45 min of He-GDC. The first ECRH plasma operation took place after 50 min of H_2-GDC. The last H_2-GDC was performed before the last operations week of the campaign. The impurity partial pressures develop along a single envelope curve from H_2-GDC to H_2-GDC. ECRH operation as well as He-GDC clearly has little effect on the overall removal trend. This can be understood from a localized plasma surface interaction area in the diverted plasmas and the absence of chemical processes in He-GDC. The presence of impurities on the surfaces in the first operation days did not prevent operating W7-X close to the set energy limits. Nevertheless, impurity radiation in the plasma was high, density control in H_2 was challenging and radiative collapses occurred frequently.

3. Wall desaturation by Helium conditioning

3.1. Gas balance

Fig. 3 plots the pumped amount of gas vs. the injected amount of gas for all experiments in OP1.2a. It clearly illustrates that generally H_2 discharges (blue markers) feature net retention while He discharges (red markers) have net removal. The analysis includes the gas introduced via valves as well as inboard and outboard launched pellets. The pumped gas amount is obtained by time integrating the gas pressure, an averaged signal from 20 gauges located in the pumping ducts, multiplied by the effective pumping speed for He and H_2. The pumped gas is assumed to be either all He or all H_2 in respective He and H_2 pulses. This approach is justified in this plot as it overestimates the pumped amount in H_2 pulses in case of impurities outgassing. Impurities are pumped at a lower rate than H_2. It also overestimates the pumped amount in He pulses in case of H_2 outgassing but only slightly; He is pumped about 10% faster than H_2.

The net retention in H_2 discharges is explained by trapping of hydrogen in He-conditioned walls, codeposition with eroded material and

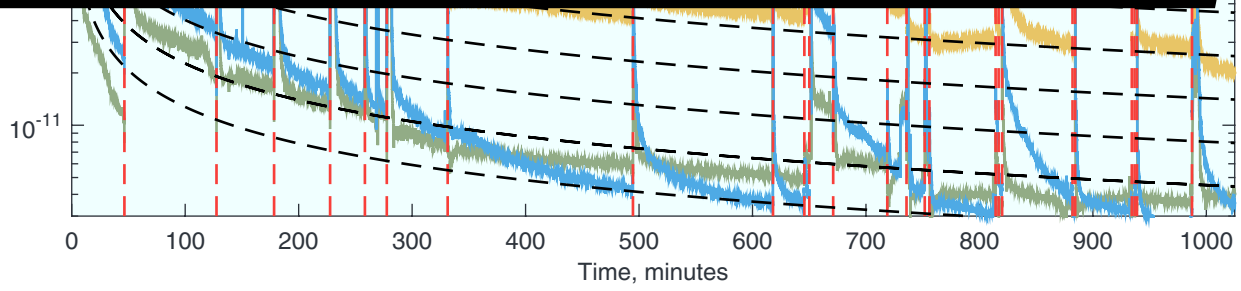

Fig. 2. Mass spectrometry intensities for subsequent H_2-GDC's procedures from campaign start to end as function of cumulated H_2-GDC time. The black dashed grid lines show time dependency ($t^{-0.7}$), the red dashed lines indicate ECRH operation days.

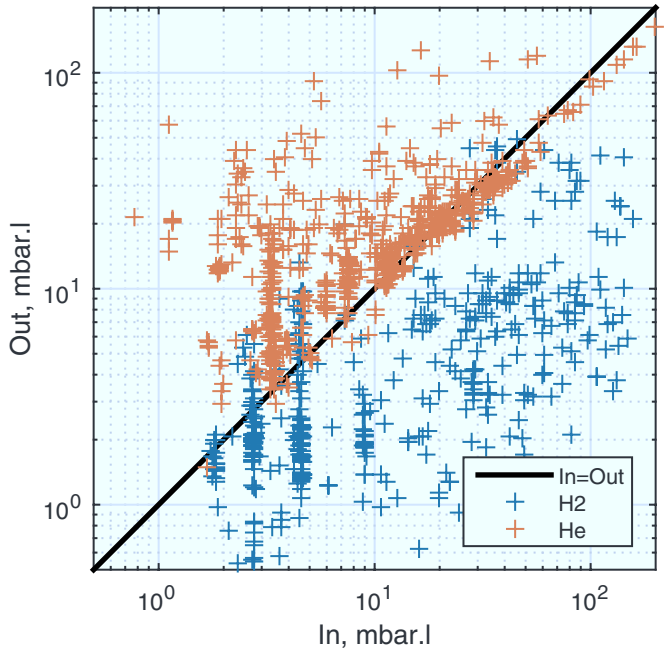

Fig. 3. Gas balance for all ECRH experiments of OP1.2a. He and H_2 discharges are shown as red and blue markers respectively.

implantation in the PFC. Net removal in He discharges is understood from complete recycling of helium and additional plasma induced desorption of hydrogen. These phenomena, known and observed on many fusion devices with carbon PFC [9], make controlling the hydrogen content in the PFC's throughout an operational day rather challenging. It is nevertheless needed in order to control the plasma density, a prerequisite for stellarator operation. The limited efficiency of plasma core fueling by OP1.2a main gas valves makes controlling the fuel recycling at the plasma facing components particularly important [10]. Fig. 4 shows density, feedback gas flow and manometer pressure

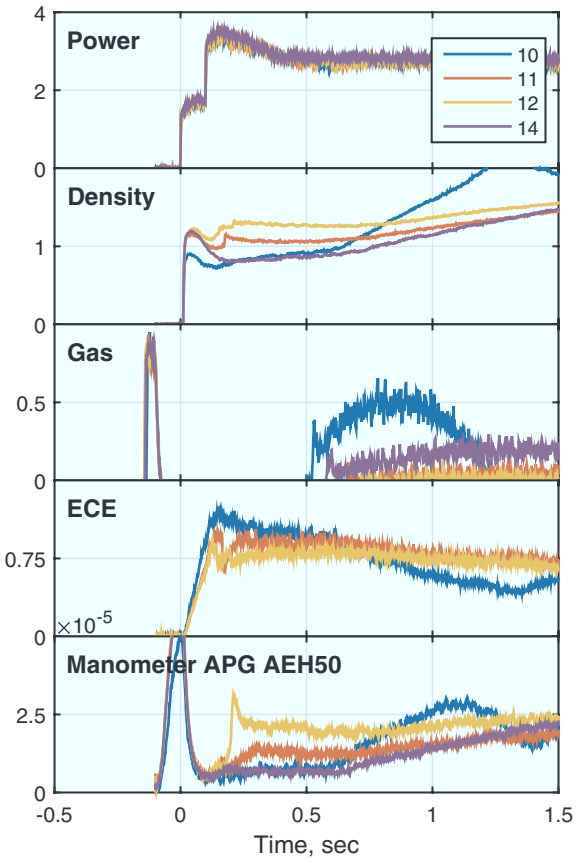

Fig. 4. Effect of wall saturation in subsequent H_2-ECRH pulses EX20171121 [10–12] on density, feedback controlled gas flow, ECE temperature and manometer pressure. Illustration of recovered conditions in pulse following He conditioning EX20171121.14.

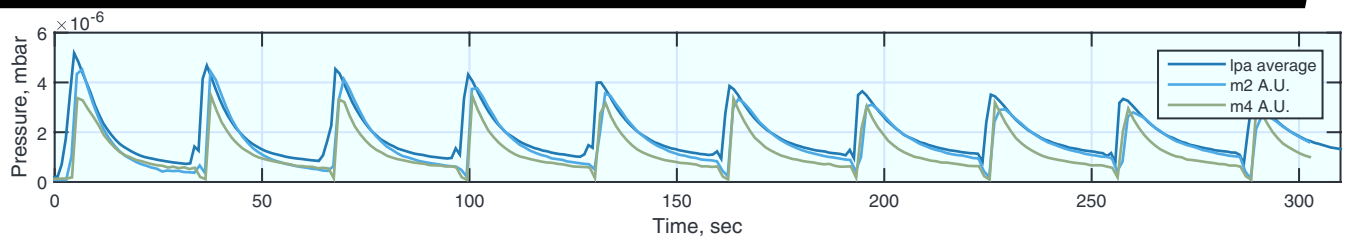

Fig. 5. Conditioning sequence EX20171121.39 consisting 10 pulses of 1.5 s at modest power of 1.5 MW with 30 s pulse interval. Ongoing recovery is apparent from interferometry density, ECE temperature, passive spectroscopy for hydrogen, carbon and oxygen, and H_2 partial pressure QMS.

of 4 subsequent H_2 discharges on W7-X with identical ECRH power and gas prefill. Clearly density increases, gas consumption decreases, ECE temperature decreases and in-vessel gas pressure by manometers [11] increases in the first 3 H_2 pulses. The 4th pulse (ECE not available), preceded by a recovery discharge in He (not shown), recovered initial conditions of the 1st pulse. The effect is most visible in time window 0.1–0.6 s where the gas prefill is complemented by wall fuelling only.

3.2. Helium ECRH conditioning

Two types of He ECRH wall conditioning procedures were studied in the first divertor campaign of W7-X: (i) medium to high energetic "single He recovery discharges" and (ii) sequences of 10–20 short low to medium power discharges with fixed duty cycle, labelled as "pulse trains". The latter type is found most efficient in terms of removal [12]. The interferometry density, QMS H partial pressure and characteristic radiation for hydrogen, carbon and oxygen from passive spectroscopy decreases from pulse to pulse while the ECE temperature increases, indicating the progressing conditioning (Fig. 5). Performing short discharges with idle time between pulses for evacuating the removed gas reduces also the migration and redeposition of H or impurities during the conditioning discharge procedure [13]. Each of the 10 pulses in the sequence shown in Fig. 5 had a short duration of 1.5 s at modest power of 1.5 MW. The pulse lengths (1–5 s) and the time interval between ECRH pulses (10–60 s) will be subject for further optimization in the next campaign.

When the wall is strongly loaded, i.e. when He-conditioning is required, naturally outgassing will be strong and a radiative collapse during the conditioning discharge can be a concern. A radiative collapse occurs (i) when the plasma density approaches the empirical density limit $n_e \sim P^{0.5}$ [14] or (ii) when a negative power balance in the plasma core or locally in the edge crushes the plasma-stored energy. Cooling of the plasma center may originate from impurity accumulation or over-fueling (e.g. by pellets) while edge cooling may follow additionally from strong outgassing combined with poor core fueling efficiency. It is experienced that the single He recovery discharges which are generally longer (> 3 s) and use higher power (> 3 MW) compared to the pulse train discharges (< 2 s and < 3 MW) are more prone to a radiative collapse. This is in agreement with earlier limiter operation observations where the achievable pulse length is determined by the injectable energy [7]. For same poor wall conditions one can sustain a high power discharge for a short duration, or a low power discharge for a long duration. Modelling this effect by 0D particle and energy balances is however not straightforward; it requires describing the exchange of particles and energy between the plasma core, the plasma edge and the PFC's which all may involve non-linear effects, such as surface temperature effects at the PFC. When a radiative collapse occurs in a single conditioning discharge, a second He pulse is required from experience. Conditioning by pulse trains generally allows for more efficient use of the experimental time on W7-X.

3.3. Helium GDC

The total net hydrogen retention in the first 3 pulses shown in Fig. 4 amounts to 124 mbar.l. These discharges were the first H_2 pulses following a 20 min He-GDC procedure. The single He recovery discharge, though recovering conditions for the next hydrogen pulse, removed only 11 mbar.l of hydrogen (Table 1). Although He-ECRH conditioning was further optimized to maximize removal, favoring pulse trains as best procedure, it is experienced that He-GDC between experimental days is still much needed to offset the hydrogen inventory build-up in the PFCs throughout an operation day as well as to avoid the accumulation of impurities. The duration of the He-GDC procedures ranged from 20 to 45 min at 1–1.5 A per anode, 210 V and 3.8×10^{-3} mbar. The optimization of the procedure is presented in [12]. The GDC is ignited in H_2, as this is more stable given the maximum allowed anode voltage of 3 kV and achievable pressure of 5×10^{-2} mbar. Within 5 min hereafter, the working gas is changed to helium. This procedure

Table 1
Illustration of H_2 and He gas balance of 5 subsequent pulses.

Experiment		Retention, mbar.l	
#	Gas	H_2	He
Ex20171121.10–12	H_2	124	−15.5
Ex20171121.13	He	−11	−2.4
Ex20171121.14	H_2	6.5	−3

ture
time
ssure
ature.
fter it
a pulse.
decays
emingly
s. Due to

through charge exchange or dissociation neutrals. If this is the case, then hydrogen and impurity accumulation on these (cold) stainless steel panels throughout an operational day may likewise be a concern, requiring dedicated conditioning efforts throughout the day; e.g. by ICRF conditioning or boronization. Finally also erosion of stainless steel by He-GDC was observed when comparing characteristic radiation spectra of before and after the He-GDC [12].

4. Wall temperature and outgassing

4.1. Impurity outgassing

As a result of passive cooling to ambient temperature (~28 °C) significant variations in the PFC temperature throughout an operational day are observed. Thermocouples (TC) that monitor the graphite tiles and underlying support structure of the divertor registered temperatures up to 526 °C. Fig. 6a shows a typical divertor temperature evolution throughout an operational day for the 40 (of 160) most responsive TC locations (separate black lines). It is immediately clear that there are large temperature gradients along the components. Some locations heat up strongly during an ECRH discharge, indicated by red (He) and blue (H_2) vertical dashed lines, adding up to 100 °C to the initial temperature. The highest temperature difference, final minus the high discharge repetition rate on W7-X this results in a CO background pressure increase of about one order of magnitude during the day. The increase of the oxygen content in the neutral gas will be mitigated in future campaigns on W7-X by active cooling of the PFC's, by applying boronization to getter the oxygen, and discharge conditioning such as H_2-GDC or ICRF conditioning. Deliberate heating of the divertor by ECRH discharges can be considered as localized baking tool. The highest energy throughput is achievable by applying pulse trains.

4.2. Hydrogen outgassing

The PFC temperature naturally also affects the recycling of hydrogen during a plasma discharge and the continued outgassing after a discharge. Repeating identical pulses, in case of actively cooled PFC, one expects the hydrogen outgassing to increase from pulse to pulse due to a progressing saturation of the PFC's. Once saturation is achieved the outgassing stays constant. Fig. 7 shows the outgassing of a series of 23 nearly identical pulses of 2 s duration, with 2.5 MW ECRH power and 6 mbar.l injected H_2 gas. The time axis zero point is set at the discharge termination. The total outgassing from pressure gauges and hydrogen outgassing from QMS is given on Fig. 7a and 7b respectively. The averaged temperature throughout the pulse, calculated as in Fig. 6a, is indicated as a subplot with same color-coding as the pressure time

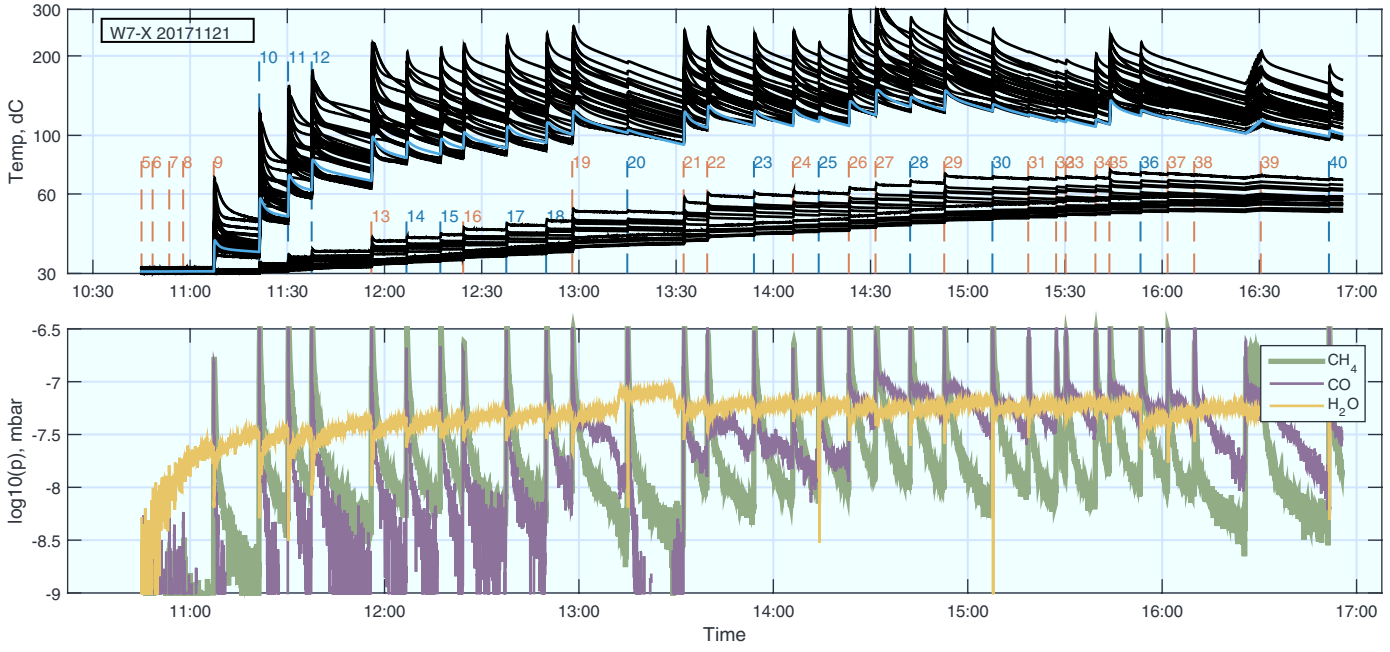

Fig. 6. Divertor temperature from thermocouples (top) and impurity outgassing from QMS (bottom) throughout an operational day (20,171,121). Vertical dashed lines in top figure indicate ECRH pulses: red for He-discharges, blue for H_2 discharges. The cyan line represents the averaged temperature over the 40 most responsive thermocouples (i.e. black lines).

Fig. 7. Outgassing after a pulse for a series of 23 nearly identical pulses as function of the wall temperature (Ex20170920.04–26). Left: total outgassing from pressure gauges, center: hydrogen outgassing from QMS, right: simulated outgassing. Wall temperature in each pulse is given in as sub-axes on the left plot indicating the color-coding of the pressure time traces.

traces. While the material temperature increases from pulse to pulse, the outgassing pressure peaks decrease. Although simulating global outgassing measurements by local outgassing is generally challenging, basic modelling can reproduce the hydrogen outgassing dependence as a temperature effect. A recombination–diffusion model is often used to describe hydrogen outgassing from PFC's [17]. Such model considers (i) atomic hydrogen implantation near the surface, (ii) atomic hydrogen diffusion inside of the material and (iii) hydrogen recombination at the material surface. The outgassing rate $q(t)$ is given by

$$q(t) = \frac{D}{2}\left(\frac{\partial u}{\partial t}\right) = K_r u^2$$

with u the hydrogen density at the surface, $D = D_0 \exp(-E_D/kT)$ the effective diffusion coefficient with T the material temperature, $E_D = 0.4$–0.9 eV the energy barrier for hydrogen jumps between two lattice points and $D_0 = 10^{-11}$–10^{-4} m^2/s [18], and $K_r = K_0 \exp(-E_R/kT)$ the recombination coefficient. Fig. 7c shows a tentative outgassing simulation of the 23 subsequent pulses with $D_0 = 5 \times 10^{-6}$ m^2/s and $E_D = 0.6$ eV. The surface interaction area is fixed at 10 m^2, the approximate plasma wetted area at the island divertor. The recombination coefficient $K_0 = 4.5 \times 10^{-6}$ m^4/s and $E_R = 0.35$ eV are fitted to reproduce the pressure outgassing trend and correspond closely to the reported $K_r = 5 \times 10^{33}$ m^4/s on JET at 320 °C [19], while the resulting particle flux entering the surface (~6 nm), equals 6.5×10^{18} m^2/s. The simulation reproduced the pulse-to-pulse decrease of the pressure peak as observed in both total pressure and the hydrogen pressure from QMS. The outgassing tail increases with increasing wall temperature for both the total pressure and the simulation while this is much less pronounced for the measured hydrogen pressure. The absolute values of the simulated hydrogen pressure tails correspond better to the measured hydrogen pressure than to the total the pressure.

5. Conclusion

Controlling the recycling of hydrogen and the release of impurities from the plasma facing components proved to be essential and challenging throughout the first divertor campaign on W7-X. One week of baking at 150 °C was applied before the campaign to successfully desaturate the PFC's from water and hydrocarbons, followed by 50 min of H_2-GDC to remove mainly carbon oxides. Removal in these both procedures follows an approximate $t - 0.7$ dependency, except for methane that is continuously produced by chemical sputtering in H_2-GDC. Neither ECRH plasma operation nor He-GDC operation significantly affect the observed t − 0.7 envelope curve that continues over the total 16.5 h of H_2-GDC during the campaign. In future campaigns, extensive GDC operation will be performed before ECRH plasma operation as GDC in H_2 is now fully commissioned.

H_2 ECRH discharges are shown to feature net retention while He discharges have net removal. Experimental programs in hydrogen are therefore interlaced with He discharges to desaturate the wall from hydrogen, recover good recycling conditions and hence establish plasma density control. Optimized He ECRH wall conditioning procedures consisted of sequences of 10–20 short low to medium power discharges with fixed duty cycle. These discharges experienced a low probability for a radiative collapse, which would cancel the remainder of the procedure. The time between pulses serves to evacuate the wall-released gas mitigating migration and redeposition. He-GDC remained needed between each experimental day to fully offset the hydrogen inventory build-up. The He-GDC removes as well impurities such as CH_4, CO and CO_2. Drawbacks of this procedure are however He retention in the stainless steel panels as well as sputtering and redistribution of stainless steel components. Substituting He-GDC by ICRF conditioning may be studied in future.

A significant increase in the averaged divertor temperature is observed throughout an operational day as a result of the passive cooling to ambient temperature. The H_2O background pressure increases approximately proportional to the averaged TC temperature. CO outgassing seemingly relates to the temperature of the hottest TC locations. The increase of the oxygen content in the neutral gas affects plasma operation. It will be mitigated in future W7-X campaigns by applying boronization to getter the oxygen, by active cooling of the PFC's, and by discharge conditioning such as H_2-GDC or ICRF conditioning. The PFC temperature also affects recycling of hydrogen. Preliminary recombination-diffusion modelling of hydrogen outgassing suggests enhanced diffusion to deeper surface layers with increasing wall temperature, which results in better wall pumping. This indicates that the experienced plasma performance degradation throughout an operational day results from increased impurity outgassing at higher wall temperature rather than hydrogen saturation of the wall.

Conflict of Interest

The authors declare that they have no known competing financial interests or personal relationships that could have appeared to influence the work reported in this paper.

Acknowledgements

This work has been carried out within the framework of the EUROfusion Consortium and has received funding from the EURATOM